Isotope fractionation of diethyl phthalate during oxidation degradation by persulfate activated with zero-valent iron

Ning Min, Jun Yao, Langping Wu, Meseret Amde, Hans Hermann Richnow, Yafei Chen, Chaochang Wu, Hao Li

PII: S1385-8947(21)03711-6
DOI: https://doi.org/10.1016/j.cej.2021.132132
Reference: CEJ 132132

To appear in: *Chemical Engineering Journal*

Received Date: 27 March 2021
Revised Date: 26 August 2021
Accepted Date: 27 August 2021

Please cite this article as: N. Min, J. Yao, L. Wu, M. Amde, H. Hermann Richnow, Y. Chen, C. Wu, H. Li, Isotope fractionation of diethyl phthalate during oxidation degradation by persulfate activated with zero-valent iron, *Chemical Engineering Journal* (2021), doi: https://doi.org/10.1016/j.cej.2021.132132

Isotope fractionation of diethyl phthalate during oxidation degradation by persulfate activated with zero-valent iron

Ning Min[a], Jun Yao[a,*], Langping Wu[b], Meseret Amde[a,c], Hans Hermann Richnow[d], Yafei Chen[a], Chaochang Wu[a], Hao Li[a]

[a]School of Water Resources and Environment, Research Center of Environmental Science and Technology, Sino-Hungarian Joint Laboratory of Environmental Science and Health, China University of Geosciences (Beijing), 29 Xueyuan Road, Haidian District, 100083 Beijing, China

[b]Department of Civil and Mineral Engineering University of Toronto 35 St. George Street. Toronto, ON M5S 1A4, Canada

[c]Department of Chemistry, College of Natural and Computational Sciences, Haramaya University, Oromia, Ethiopia

[d]Department of Isotope Biogeochemistry, Helmholtz Centre for Environmental Research – UFZ, Permoserstraße 15, Leipzig 04318, Germany

*Corresponding author:

E-mail: yaojun@cugb.edu.cn

Phone: +86-10-82321958

Fax: +86-10-82321958

Abstract:

This study reports the ^{13}C and ^{2}H isotope fractionation associated with the oxidation of diethyl phthalate (DEP) by persulfate (PS) activated with zero-valent iron (ZVI) using three concentration levels (0.2, 0.5 and 1.0 g L^{-1}) at different pH values, 3, 7 and 11, respectively. The results showed that the degradation of DEP followed a pseudo first-order kinetics. The fastest degradation was found at neutral conditions (pH 7). Similar carbon and hydrogen isotope fractionation (ε_C and ε_H) was observed during the oxidation of DEP by ZVI activated PS at pH 3, 7 and 11. At ZVI concentration of 0.5 g L^{-1}, the correlation of ^{13}C and ^{2}H fractionation (Λ) were obtained to be 12.7 ± 3.5, 11.1 ± 4.2 and 12.0 ± 2.9 at pH 3, 7 and 11, respectively. The concentration of ZVI has no effect on the correlation of ^{13}C and ^{2}H fractionation (Λ). In addition, radical quenching approach and electron paramagnetic resonance (EPR) were combined to explore the dominant radical species in the ZVI activated PS reaction, and hydroxyl radical (•OH) was found to be the predominant radical at all pH studied. The results of CSIA show the addition of •OH to the aromatic ring of DEP is the main reaction mechanism, which is consistent with the results of radical quenching experiment and EPR study. Carbon and hydrogen apparent kinetic isotope effects (AKIEs) obtained from •OH reactions with DEP supported the hypothesis of C-H bond cleavage. Thus, carbon and hydrogen isotope enrichment factors clearly distinguish the different reaction mechanisms and hence, are a promising approach to improve understanding of radical species reaction pathways for chemical oxidation of DEP.

Key words: Compound-specific stable isotope analysis; Diethyl phthalate; Persulfate; Carbon and hydrogen isotopic fractionation; Zero-valent iron

1. Introduction

Phthalates (PAEs) are a class of hydrophobic organic substances with large production volume and wide application[1, 2]. They are widely applied in mineral processing as flotation agents, and used as plasticizers, pesticide carriers, cosmetics, coatings, and others [3, 4]. The applications in China's non-ferrous metal mines are complex and difficult to address[5]. With the expansion of large-scale mining, poor ore has become the main source of mineral extraction, so large amounts of organic flotation reagents including PAEs have been used to extract the target metals[6].

Diethyl phthalate (DEP) has a good emulsification effect on hydrocarbon based oils. The long-lasting foaming property and good fluidity at low temperature make DEP beneficial to the recovery of molybdenum as well as copper-molybdenum ore and thus has been used as the main foaming agent for processing of these ores [7]. Due to the lack of corresponding regulatory policies, a large amount of DEP is released into the environment[6]. DEP is classified as Substances of Very High Concern (SVHC) because of its carcinogenic and teratogenic effects and its high persistence in the environment. Metabolites and degradation products of DEP may have adverse effects on human health, especially the liver, kidneys and testes, and may also cause endocrine disorders[8-11]. At present, the hazards of DEP in mine tailings have not received widespread attention. However, the contamination may cause great damage to the ecological environment and pose a huge potential risk to human health[12]. In Europe, regulations prohibiting products containing certain phthalates have been

implemented since 2000[13]. According to the United States-Environmental Protection Agency (US-EPA) diethyl phthalate (DEP) has been included in the list of priority pollutant[14] and the agency set the threshold limit values of DEP at 0.55 mg L^{-1} in drinking water [15].

In very recent, various methods including adsorption[16-18], biodegradation[19-25] and advanced oxidation processes (AOPs) such as Fenton oxidation, UV photolysis, photocatalytic and persulfate oxidation [26-35] have been used to treat PAEs based pollution. However, due to its ethyl groups and the lack of light adsorption at wavelengths >300 nm[36], DEP is resistant to the biodegradation and photolytic degradation. In recent years, sulfate radicals based AOPs has been used for the abatement of persistent organic pollutants (POPs)[32]. The highly reactive $SO_4^{\bullet-}$ can be generated by activation of persulfate (PS) *via* heat, metal ions, and transition metals[26]. Zero-valent iron (ZVI) is one of the most promising transition metals, which has attracted more attention on PS activation to generate $SO_4^{\bullet-}$. Reactions involving in Fe(0)/PS process are illustrated in Eq. (1) and (2)[37, 38]. Hydroxyl radicals can be formed under alkaline conditions according to Eq. (4-5)[39], $S_2O_8^{2-}$can reacted with H^+ forming sulfate radical under acidic condition based on Eq. (6-7)[40], which may also contribute to the oxidation of PAEs. *In situ* chemical oxidation (ISCO) is a promising technique for the removal of organic contaminants in soil, groundwater and aquifers[41-43]. In addition, ZVI may present in beneficiation of wastewater and tailings[6, 44] or can be added for example as micro/nanoparticle of low environmental concern. Therefore, ZVI is a reasonable activator of PS to remove DEP in ore dressing wastewater and

tailings, achieving the purpose of *in-situ* remediation. On the other hand, knowledge about the degradation processes is necessary to develop ZVI/PS remediation techniques for an efficient and economical removal of DEP in the environment. However, the degradation mechanism of DEP by ZVI activated PS (ZVI/PS) at different pH is still unclear.

$$Fe(0) + S_2O_8^{2-} \rightarrow Fe^{2+} + 2SO_4^{2-} \quad (1)$$

$$Fe(0) + 2S_2O_8^{2-} \rightarrow Fe^{2+} + 2SO_4^{2-} + 2SO_4^{\bullet-} \quad (2)$$

$$Fe^{2+} + S_2O_8^{2-} \rightarrow Fe^{3+} + SO_4^{2-} + SO_4^{\bullet-} \quad (3)$$

All pHs: $SO_4^{\bullet-} + H_2O \leftrightarrow \cdot OH + H^+ + SO_4^{2-}$ (4)

Alkaline pH: $SO_4^{\bullet-} + OH^- \rightarrow SO_4^{2-} + \cdot OH$ (5)

Acidic pH: $S_2O_8^{2-} + H^+ \rightarrow HS_2O_8^-$ (6)

$$HS_2O_8^- + e^- \rightarrow SO_4^{\bullet-} + SO_4^{2-} + H^+ \quad (7)$$

$$Fe^{2+} + O_2 = Fe^{3+} + O_2^{\bullet-} \quad (8)$$

Compound-specific stable isotope analysis (CSIA) is one of the powerful techniques that can be used to study the transformation of organic contaminants based on isotope fractionation approach[45]. The measurement of stable isotope ratios of carbon, hydrogen, and other elements has proven to be useful in the evaluation of environmental processes[46, 47]. The isotope fractionation of individual compounds can often be rationalized in terms of bonding changes in the first irreversible reaction step and is therefore a valuable approach for determining the type of reaction that initiates contaminant degradation[48, 49]. Hitherto, the carbon and hydrogen isotope fractionation of DEP has been studied for characterizing its abiotic hydrolysis, aerobic

biodegradation and oxidation by heat activated PS[36, 50]. However, there are few reports related to the isotope fractionation associated with the activation of PS by ZVI. In addition, ZVI existing in iron ore can be used as an efficient activator to promote the elimination of DEP, which gives a new possibility to the treatment technology of phthalate esters in tailings environment. It should be also mentioned that there are some reports on the degradation mechanism of DBP by PS activated with heat, UV and transition metal. But the reports did not apply CSIA to thoroughly discuss the degradation mechanism and characterize the chemical bond breakage during the reaction processes (Table S1). Hence, we believe that the current work is a novel contribution to enhance our knowledge on the reaction mechanisms. This may be essential for the application of stable isotope techniques to identify and quantify the removal of DEP by AOPs in remediation applications.

Therefore, the objectives of this study were: (i) to quantify the degradation kinetics of DEP in ZVI/PS system at different initial pHs (3, 7 and 11), (ii) to identify the DEP degradation intermediates in ZVI/PS system using GC-MS, (iii) to characterize the ^{13}C and ^{2}H isotope fractionation associated with DEP oxidation by ZVI/PS in order to explore the potential to monitor the progress of degradation using isotope fractionation in field studies and (iv) to calculate the apparent kinetic isotope effects (AKIEs) of DEP in order to explore the potential of CSIA for characterizing the radical reactions with DEP. Furthermore, isotope enrichment factors, ε_C and ε_H, for all reactions have to be determined for the characterization of degradation pathways and subsequent quantification of degradation reaction in field studies.

2. Materials and methods

2.1. Chemicals

Analytical grade DEP (purity, 99.5%), sodium persulfate ($Na_2S_2O_8$, purity, 99.9%), nano zero-valent iron (purity, 99.9%), 5,5-dimethyl-1-pyrrolinen-oxide, starch indicator (I_2, AR), potassium iodide (KI, 99.5%), sodium thiosulfate ($Na_2S_2O_3$, 99.5%), 1,10-phenanthroline monohydrate ($C_{12}H_8N_2$, 99%), sodium acetate solution (CH_3COONa, 99.8%), sulfuric acid (H_2SO_4, 95–98%) and sodium hydroxide (NaOH, 98%) were obtained from Aladdin Chemical Reagent Co., Ltd. (Shanghai, China). HPLC grade dichloromethane, methanol, ethanol (EtOH) and *tert*-butyl alcohol (TBA) were supplied by Beijing MREDA Technology Co., Ltd. (Beijing, China). Deionized water produced by a Milli-Q system (Millipore, Billerica, MA, USA) was used to prepare all experimental solutions.

2.2. Experimental procedures

Batch experimentation was conducted in triplicate to analyse the sodium persulfate oxidation reactions in a series of 500 mL flasks. $Na_2S_2O_8$ was used to generate $SO_4^{\bullet-}$ at pH 3, 7 and 11. The pH value was adjusted using H_2SO_4 and NaOH solutions, and all experiments were carried out at room temperature (20±1 ℃). Considering low solubility of DEP in water and to achieve adequate signal intensity for isotope measurements, initial concentration of DEP was set 0.8 mM. The molar ratio of PS and DEP was 100:1, and the concentrations of ZVI were 0.2, 0.5 and 1 g L^{-1}, respectively. Control experiments were conducted without the addition of PS or

ZVI, and without the addition of both PS and ZVI under identical conditions (pH 3, pH 7 and pH 11), simultaneously. To investigate the degradation kinetics of DEP, 0.5 mL reaction solution was transferred at different time intervals into 2 mL brown glass vials for HPLC analysis of the remaining DEP concentration. As a free radical quencher, 0.5 mL methanol was added to the brown glass vials in order to stop the radical oxidation reaction after sampling.

To estimate the main radical species generated in ZVI/PS system at the considered pH, radical quenching experiments were separately carried out in the presence of EtOH and TBA. EtOH and TBA, which act as radical scavengers, were added to obtain a concentration of 400 mM, which corresponded to a 500:1 molar ratio compared to the DEP. The second order rate constant value of •OH with TBA is $6 \times 10^8\ M^{-1}s^{-1}$, which is almost 3 orders of magnitude faster than that of $SO_4^{\bullet-}$ with TBA ($4\times 10^5\ M^{-1}s^{-1}$)[42]. Therefore, TBA is usually used as a chemical probe to completely quench •OH but only some amount of $SO_4^{\bullet-}$. EtOH can quench $SO_4^{\bullet-}$ and •OH, simultaneously. In addition, electron paramagnetic resonance (ESR) experiments were conducted to identify the radical species using 5,5-dimethyl-1-pyrrolinen-oxide (DMPO) as a spin-trapping agent. In brief, a suspension containing 1 mL of 0.1 M DMPO solution was spiked into the reaction solutions at different time intervals and further shaked for 1 min [51]. Then, the suspension was filtered through a 0.22 μm MCE syringe filter and analyzed on a Bruker EMS Plus X-band ESR spectrometer at room temperature [52].

To evaluate the isotope fractionation pattern of DEP in the ZVI/PS system, the remaining DEP fraction at different time intervals was extracted from the aqueous solution with 5 mL of dichloromethane. The extracts were concentrated to 2 mL for carbon isotope analysis, and then were concentrated to 200 µL for hydrogen isotope analysis.

2.3. Concentrations, intermediate products and isotope analysis

The concentrations of DEP in all experiments were measured by an UltiMate 3000 HPLC system (Thermo Fisher Scientific, USA) equipped with a UV detector at 253 nm. A reversed-phase C_{18} column (250 mm length x 4.6 mm internal diameter, 5.0 µm particle size) was used for separation and the temperature was maintained at 30 ℃. The mobile phase was a mixture of methanol and ultrapure water (65:35, *v:v*) with a flow-rate at 1 mL min^{-1}. The DEP concentrations were calculated using an external calibration curve obtained from the HPLC measurements at identified retention time (t_R = 6.59 min) (Fig. S1).

An Agilent GC-MS (7890B-5977B) system (Agilent, USA) was used to investigate reaction products of the DEP. A DB-5 column (30 m x 0.25 mm x 0.25 µm) (Agilent, USA) was used to separate the compounds. The oven temperature program was 60 ℃ (held 1 min) followed by a ramp of 8 ℃/min to 295 ℃ (held 3 min). The carrier gas was helium (1 mL min^{-1}) and each 1 µL sample was injected in split mode with a split ratio of 20:1 and the injector temperature was set at 280 ℃. The GC-MS spectrum of DEP and reaction product are shown in Fig. S2 and the mass spectrum of the identified degradation product is given in Fig. S3.

Carbon and hydrogen isotope compositions of DEP were measured by a DELTA V gas chromatography-isotope ratio mass spectrometer (GC-IRMS, Agilent, USA). Samples were injected in split mode (20:1, 1 μL) for carbon isotope measurement, and splitless mode was applied for hydrogen isotope analysis to obtain optimum signal intensity. Good peak shape of DEP was achieved using a DB-5MS column (30 m x 0.25 mm x 0.25 μm) (Agilent, USA). The GC oven temperature program and other GC parameters were identical to the ones as in GC-MS (see above GC-MS procedure). Reproducibility of $\delta^{13}C$ and $\delta^{2}H$ values was monitored by triplicate injections for each sample. The uncertainties of isotope analysis were within the typical range of analytical uncertainties ($\delta^{13}C$: ± 0.5‰, $\delta^{2}H$: ± 5‰). The GC-IRMS spectrum of DEP were shown in Fig. S4.

2.4. Persulfate and Fe^{2+} determination

Colorimetric method was used to determine the PS concentration using iodide as reported elsewhere[53]. The concentration of Fe^{2+} in the studied system was determined by o-phenanthroline spectrophotometry. Briefly, 10 mL o-phenanthroline aqueous (0.2 %) solution and 5 mL sodium acetate solution (10 %) were added to a 25 mL colorimetric tube and shaken. Then 1 mL of samples was added to the colorimetric tube and dilute to 25 mL. The concentration of Fe (II) in the sample was analyzed by spectrophotometer at 512 nm. And the stability of the Fe^{2+} o-phenanthroline complex in the presents of persulfate was analyzed under similar conditions as used for concentration measurement in the experiments.

2.5. Isotope data evaluation

2.5.1. Evaluation of isotope fractionation

The carbon and hydrogen isotope enrichment factors (ε_C and ε_H) of DEP were determined using the Rayleigh equation, Eq. (9)[54],

$$\frac{\delta_t + 1}{\delta_0 + 1} = (f)^{\varepsilon} \quad (9)$$

where δ_t and δ_0 are the isotope compositions of substrate at time t and zero, f is the remaining fraction of substrate at time t ($f = C_t / C_0$), and ε was obtained as the bulk isotope enrichment factor.

The correlation of the shift of the hydrogen isotope ($\Delta\delta^2H$) at time t and zero and the shift of the carbon isotope ($\Delta\delta^{13}C$) during the experiment were calculated as shown in Eq. (10). The slope (Λ) was used to discriminate the reaction mechanism of the same compound.

$$\Lambda = \frac{\Delta\delta 2\mathrm{H}}{\Delta\delta 13\mathrm{C}} \approx \frac{\varepsilon_H}{\varepsilon_C} \quad (10)$$

2.5.2. Apparent kinetic isotope effect (AKIE) calculation

The ε values were calculated by Rayleigh equation (Eq. 9) using bulk isotope data, which was used to calculate the position-specific intrinsic isotope effect associated with the particular bond change reaction[55]. Conversion of the observable ε value to AKIE (Eq. (11)) is needed to characterize the chemical bond breaking mechanism and degradation pathway[56].

$$AKIE = \frac{1}{1 + \frac{n}{x}z \cdot \varepsilon_{bulk(}(‰)/1000} \quad (11)$$

Where ε bulk is the bulk isotope enrichment factor, n is the number of atoms of the element in the molecule, x is the number of atoms at reactive positions and z is the number of indistinguishable reactive positions.

3. Results and discussion

3.1. Degradation kinetics of DEP at different pHs

The chemical oxidation processes of DEP although a second order reaction followed first order kinetics at all pHs (pH 3, 7 and 11) ($R^2 \geq 0.9337$, Table 1), which is consistent with the previous studies. Along with the increasing ZVI concentration of 0.2, 0.5 and 1 g L^{-1}, rate constants (k) of DEP degradation in the ZVI/PS system increase from 0.0035, 0.0095, and 0.0301 h^{-1} at pH 3, to 0.0059, 0.0115 and 0.0306 h^{-1} at pH 7, and to 0.0034, 0.0044 and 0.0204 h^{-1} at pH 11, respectively (Fig. 1). Control experiments (without ZVI and PS) showed negligible decrease of DEP, and no carbon and hydrogen isotope fractionation was observed at pH 3 and 7 (Fig. S5), thus showing that ZVI concentration is the predominant factor for activation. Under alkaline conditions the control experiment at pH 11 without persulfate show that hydrolysis take place with a rate constant of 0.0028.

In addition, at pH 11 carbon fractionation has been detected with an enrichment factor of -5.90±0.71, indicating isotope fractionation upon alkaline hydrolysis of DEP is consistent with previous studies [56, 57] (Fig. S6, Table S2). This shows that at pH 11 in addition to radical oxidation hydrolysis need to be taken into account.

Control experiment (with PS and without ZVI) at pH =3 and pH =7 showed slight decrease in concentration of DEP in the first 30 minutes, but remained stable in the DEP/PS system after 30 minutes. The main reason may be that PS initially produces free radicals, and due to lack of activator, the free radicals in the experiment get consumed, and the concentration of DEP become stable (Fig. S7).

Table 1 here

Figure 1 here

The results also showed that under acidic, neutral and alkaline conditions, the degradation rate of DEP increased with the increase of ZVI concentration. In addition, the degradation rate of DEP in ZVI/PS system at pH 7 is faster compared to acidic (pH 3) and alkaline (pH 11) conditions, and the lowest degradation rate was observed under the acidic condition.

3.2. Decomposition of persulfate and the concentration of Fe^{2+}

3.2.1. The concentration of PS in the presence of ZVI but without DEP

In order to understand the effect of ZVI on the decomposition of PS under different pH conditions, the PS concentration in the presence of ZVI but without DEP was monitored and the results are presented (Fig. 2).

Figure 2 here

The results showed that the decomposition trend of PS gradually slowed down after 60 minutes at pH = 11 (25%). However, the decomposition rate of PS in acidic (30%) and neutral conditions (29%) was higher than that in alkaline conditions, which may be the reason why the degradation rate of DEP in acidic and neutral conditions was significantly higher than in alkaline conditions.

3.2.2. Decomposition of persulfate in studied conditions

Since the main source of the free radicals in the DEP/PS/ZVI system is PS, the concentration of PS during the reaction process at different pHs have been monitored. As shown in Fig. 3, PS is gradually consumed under all pH conditions (at pH 3, 7, 11, PS consumption was about 46.5%, 48.8% and 45.2%, respectively). Similar to the trend of PS consumption, the degradation rate of DEP was highest in neutral followed by in acidic and alkaline conditions. The results show the reaction of radicals with DEP improve the consumption rate of PS.

Figure 3 here

3.2.3. The concentration of Fe(II) in studied conditions

The concentration of Fe^{2+} in the DEP/PS/ZVI system was determined by o-phenanthroline spectrophotometry (Fig. 4) to investigate the reaction of ZVI to Fe(II) in the reaction system. The results indicated that the concentration of Fe(II) gradually increased as the reaction proceed which indicate that ZVI was oxidised to Fe(II),

according to Eq. (1) and Eq. (2). With the progress of the reaction, the Fe(II) may be gradually transformed into Fe(III) (Eq. 3).

Figure 4 here

3.3. Carbon and hydrogen isotope fractionation during the chemical oxidation

Both carbon and hydrogen isotope fractionation were detected during the DEP oxidation in the ZVI/PS system. The values of carbon and hydrogen isotope compositions became less negative along with the reaction progresses, showing a normal isotope effect (Fig. S8). The carbon and hydrogen isotope enrichment factors of DEP were quantified (Fig. 5). The Rayleigh regression of DEP showed high correlation with a high coefficient of determination ($R^2 \geq 0.9205$) for δ^2H and $\delta^{13}C$, and the uncertainty was within the 95% confidence interval (C.I.). The carbon and hydrogen isotope fractionation of control experiment (with PS and without ZVI) showed the carbon and hydrogen isotopes gradually enriched in the first 30 minutes, and the carbon and hydrogen isotope enrichment factors were -1.43±0.97, -1.61±0.65, -32.96±1.2 and -26.45±1.4, respectively, which is consistent with that of degradation kinetics and the previous studies (Table 3). After 30 minutes, the carbon and hydrogen isotope values remained stable. The reason may be that with the consumption of free radicals which are limited in amount due to absence of ZVI, and the DEP concentration remained stable (Fig. S9)

Figure 5 here

The ε_C values at different concentrations of ZVI were calculated to be -1.1±0.21‰, -0.8±0.20‰, and -0.6±0.36 ‰ at pH 3, -1.10±0.01 ‰, -1.11±0.01 ‰, -1.00±0.01 ‰ at pH 7, and -1.48±0.21 ‰ , -1.18±0.20 ‰, -0.77±0.16 ‰ at pH 11, respectively (Table 2). Similarly, the ε_H values were calculated to be 10.2±3.6 ‰, 8.7±5.1, and 8.5±3.3 ‰ at pH 3, -14.0±4.1 ‰, -11.6±5.5 ‰, -13.7±3.2 ‰ at pH 7, and -23.0±3.2 ‰, -19.2±4.6 ‰, -14.0±2.1 ‰ at pH 11, respectively. The ε values obtained at different ZVI concentration at the same pH were statistically identical when considering the 95% CI, revealing an average ε_C and ε_H values of 0.79±0.45 ‰ and 8.97±4.87 ‰ at pH 3, 1.10±0.45 ‰ and 13.10±5.60 ‰ at pH 7, and 3.10±0.60 ‰ and 18.02±5.01 ‰ at pH 11, respectively.

Table 2 here

Results also showed that high concentration of ZVI (0.2 g L^{-1} to 1.0 g L^{-1}) lead to slightly low carbon and higher hydrogen fractionation compared isotope fractionation of •OH and $SO_4^{\bullet-}$ radical reaction observed in previous study (Table 3). Whereas the ^{13}C fractionation is in the same order, experiments in which persulfate is activated by heat the hydrogen fractionation is statistically lower. In contrast the pure reaction with •OH radicals give a higher ^{13}C fractionation whereas the trend for ^{2}H fractionation is lower than in most experiments with ZVI activation. This already indicate that the persulfate/ZVI system show specific fractionation pattern not identical to pure sulfate and hydroxyl radical reactions.

This may be an indicator that at high radical concentration the relative contribution of one of the radical species become more dominant. A previous study shows that •OH results in lower hydrogen enrichment factors and larger carbon enrichment factors compared $SO_4^{\bullet-}$ (Table 3). We speculate that at high radical concentration the contribution of •OH reaction become more dominant leading to a reduction of the ^{2}H fractionation and an increase of ^{13}C fractionation due to the existence of $SO_4^{\bullet-}$ in the ZVI/PS system.

At pH 3 and pH 7 the carbon and hydrogen isotope fractionation is statistically almost identical showing that a very similar mechanism is predominating. At pH 11 with the increase of ZVI concentration the ^{13}C fractionation decrease. The same trend is observed for ^{2}H fractionation (although less pronounced). This may show that at pH 11 reaction mechanism may change which might be reasonable because a contribution hydrolysis even not prominent on the overall reaction need to be take into account.

Table 3 here

The correlation of carbon and hydrogen isotopic value of DEP in ZVI/PS system were compared in dual isotope plots. In all case, ε_C values of DEP with different concentrations of ZVI showed a similar trend of carbon isotope fractionation. ε_H values of DEP showed a trend to a larger hydrogen isotope fractionation at pH 11 compared to the ones at pH 3 and pH 7. Thus, the difference of hydrogen enrichment factors may be used to identify different reaction processes. In addition, similar slope ($\Lambda=\Delta\delta^{2}H/\Delta\delta^{13}C$) were observed in all studied conditions (Fig. 6) (Λ = 15.1±4.2, 12.7±3.5 and 11.7±2.6 at pH 3, Λ = 10.9±2.9, 11.1±4.2 and 11.6±3.6 at pH 7 and Λ =

15.0±3.1, 12.0±2.9 and 12.8±2.8 at pH 11). This result suggests that the dominant radicals, which are recognized as •OH, are all the same at the studied pHs (pH=3, 7 and 11) ZVI (0.2, 0.5 and 1.0 g L^{-1}).

Figure 6 here

The Λ values fall statistically is the similar range which is clearly different from pure •OH radical reaction[36] and most similar to heat induced persulfate sulfate catalyzed reaction reactions where •OH and $SO_4^{\bullet-}$ radicals are competing[36]. This may reinforce the assumption that the ZVI/PS system show a specific reaction mode with DEP not identical to previous studies.

3.4 Identification of predominant radical species

Previous studies have shown that in the ZVI/PS system, various free radicals such as •OH[58, 59], $SO_4^{\bullet-}$ [60, 61] and $O_2^{\bullet-}$(Eq (8)) [42] may be generated and responsible for the degradation of DEP at different pHs. $SO_4^{\bullet-}$ can react with hydroxyl ion and water to generate •OH as shown in Eq. (4) and (5) [62, 63]. It is reasonable to infer that •OH presents in the reaction ZVI/PS system. To explore the main types of free radicals under different pH conditions, two alcoholic radical scavengers, TBA and EtOH, were added into the reaction system[64]. Previous studies[36, 42] show that both $SO_4^{\bullet-}$ and •OH could be quenched by EtOH. The second-order rate constant in •OH/EtOH (1.2–2.8 × 10^9 $M^{-1}s^{-1}$) system is near that of $SO_4^{\bullet-}$ / EtOH (1.6–7.7 × 10^7 $M^{-1}s^{-1}$). TBA preferentially quenches •OH due to the second-order rate constant of •OH reacting with TBA (3.8–7.6 × 10^8 $M^{-1}s^{-1}$) is nearly a factor of 10^3 greater than the rate constant of $SO_4^{\bullet-}$ with TBA (4–9.1 × 10^5 $M^{-1}s^{-1}$). The results obtained from the

quenching experiments (Fig. 7) indicate that TBA and EtOH exert a strong inhibiting effect on DEP degradation at all pHs[65-67]. Besides, EPR was applied to verify the types of free radicals in the system. DMPO can capture the two free radicals to generate the corresponding secondary products, DMPO-OH and DMPO-SO_4, which can be detected by the EPR spectrometer [68-70]. The results (Fig. 8) demonstrate that $SO_4^{\bullet-}$ and •OH coexist at pH 3 and 7, and •OH is the predominant species at these pH values. DMPO−SO_4 signal was not observed at pH 11, which show that •OH is the dominant free radicals in this condition (pH=11). The main reason may be that DMPO−SO_4 reacts with hydroxyl to form •OH.

Figure 7 here

Figure 8 here

The first-order kinetic constants of DEP in ZVI/PS/E_tOH and ZVI/PS/TBA system decreased by 80.1% and 77.9% at pH 3, 86.1% and 85.4% at pH 7 and 90.9% and 90.6% at pH 11 (Table 4), respectively, indicating that the •OH and $SO_4^{\bullet-}$ may coexist at the pH 3 and 7, and •OH may be the predominant at pH 11. Our results particularly at pH 11 are inconsistent with the previous reports, which shown •OH and $O_2^{\bullet-}$ as predominant radicals in the ZVI/PS system at pH 11[42]. Considering that there is also a reduction in phthalate concentration in the ZVI/PS/EtOH and ZVI/PS/TBA system, the possible reason is the adsorption of DEP by ZVI (Fig. S10). As the isotope composition is almost stable no bond cleavage reactions are indicated.

Table 4 here

3.5. Apparent kinetic isotope effects of DEP at different pHs

The intermediate products of DEP in the ZVI/PS and control (with PS and without ZVI) system were investigated using GC-MS analysis. Based on the molecular ion, mass fragment peak, the main possible transformation product was identified as diethyl 3-hydroxyphthalate at all studied pHs (Fig. S3)[71].

Hydroxyl radicals potentially react with dimethylphthalate in aqueous solutions by the following three pathways[72]. (i) The •OH addition leading to the radical adducts formation (RAF pathway). (ii) Hydrogen atom can be abstracted and transfer by •OH (HAT pathway). (iii) Single electron transfer to the substrate catalyzed by •OH (SET pathway)[73]. The SET pathway is endothermic and unlikely to occur due to its high energy demand (27.91 kcal / mol). However, the RAF and HAT pathways are exothermic processes (-19.41 kcal/mol to -4.97 kcal/mol), which were relatively easy to occur with an energetically preference for RAF pathway, in contrast to the addition pathway of •OH radical to the DMP ester bond carbonyl carbon (8.52 kcal/mol) which is endothermic. In this study, the hydroxyl phthalate detected in the ZVI/PS/DEP reaction system indicates the addition of •OH to the ortho-position aromatic ring of DEP. RAF is assumed to be the main reaction mechanism, which is consistent with the Gauss computational results on •OH initiated degradation of PAEs[8]. According to Eq. (11), specific apparent kinetic isotope effects (^{13}C-AKIE and ^{2}H-AKIE) were calculated according to the reactive sites in the molecule (Table 5). Experimentally determined kinetic isotope effect (AKIE) values for oxidation

reactions involving C-H bond cleavage are in the range of 1.01–1.03 for carbon isotopes and 2–8 for hydrogen isotopes[56].

Table 5 here

According to the above discussion, RAF is considered to be the main reaction pathway of DEP in ZVI/PS. For carbon isotopes, the number of carbon atoms in the molecule (n) is 12, there are two identical reaction sites of carbon atoms on the benzene ring, and there is a competitive relationship, x = 2, z = 2. For hydrogen isotopes, the total number of hydrogen atoms in the molecule (n) is 14. There are two hydrogen atoms at the benzene ring in reactive position competing for reaction (x = 2, z = 2). The ^{13}C-AKIE values of DEP in the ZVI/PS system at all pHs (pH=3, 7, and 11) were all within the expected KIE range of C-H bond oxidation (KIE_C: 1.01 - 1.03), which suggest that the C-H bond cleavage is the initial reaction step. Due to the expected hybridization change in the transition state of the benzene ring hybridization orbital, the value of $AKIE_H$ is also lower than the expected KIE_H range of the C-H bond (2-8). The $AKIE_H$ obtained in this study fell in the range of 1.14 to 1.40 (Table 3), which is consistent with the observation of Zhang et al. in which the obtained $AKIE_H$ ranged from 0.77 to 1.40 [48].

4. Conclusions

This study reports the degradation of DEP by ZVI activated PS at ambient temperature in different conditions (pH, 3, 7 and 11). The results showed that the concentration of the activator (ZVI) can affect the reaction rate but the reaction type does not change with the ZVI concentration. The radical quenching analysis and electron paramagnetic resonance (ESR) experiments indicates that •OH and $SO_4^{\bullet-}$ are all exist in ZVI/PS/DEP system at pH 3 and 7, and the proportion of •OH is relatively large. The •OH was found to be the dominant free radical in ZVI/PS/DEP system at pH 11. According to the products, diethyl 3-hydroxyphthalate, detected in the ZVI/PS/DEP reaction system, the addition of $HO^{\bullet}$ on the aromatic ring of DEP is assumed to be the main reaction mechanism. In addition, CSIA was used to evaluate the free radical degradation of DEP, the ^{13}C-AKIE and ^{2}H-AKIE values of DEP in the ZVI /PS system at all pHs (pH=3, 7, and 11) are all within the expected KIE range of C-H bond oxidation (KIE_C: 1.01 - 1.03; KIE_H: 0.77 - 1.40), which prove the C-H bond cleavage. Combining the intermediate products and carbon hydrogen isotope fractionation, the possible degradation mechanisms in studied systems have been discussed. CSIA also suggests that •OH plays a major role to oxidize DEP at all studied pH values in the ZVI/PS system. Additionally, carbon and hydrogen isotope fractionation patterns are of fundamental importance to evaluate the removal of DEP. The results of this study are an important step forward in understanding degradation mechanisms of organic compounds in the ZVI/PS system. Furthermore, the stable carbon and hydrogen isotope fractionation under different pH conditions in the

ZVI/PS/EDP system obtained in our research can, thereby, be used as a reference for evaluating field data to determine the characteristic assessment of chemical DEP conversion in the real environment. The method promises great potential for future investigations regarding the fate of DEP and can be easily applied and has great potential to analyze chemical degradation reactions in the environment using a combination of carbon and hydrogen isotope analysis.

Acknowledgements

This work has been supported partly by grants received from the National Science Foundation of China (41720104007) as well as by the project of the Major National R & D Projects for Chinese Ministry of Science and Technology (2019YFC1803500). The joint Sino-Hungarian project under contract number 2018-2.1.14-TÉT-CN-2018-00022 is, hereby, acknowledged.

Conflict of interest

The authors have no competing interest to declare.

Reference

[1]. J. Sun, J. Huang, A. Zhang, W. Liu, W. Cheng, Occurrence of phthalate esters in sediments in Qiantang River, China and inference with urbanization and river flow regime. J. Hazard Mater. 142-9 (2013) 248-249. https://doi.org/10.1016/j.jhazmat.2012.12.057

[2]. A. Suzuki, G. Teleki, Phthalate Esters as Environmental Contaminants. Nature. 238 (1972)411-413. https://doi.org/10.1038/238411a0

[3]. A Charles, D. R. P. Staples, F. Thomas, Parkerton and William J. Adams The environmental fate of phthalate esters- A literature review. Chemosphere. 35-4 (1997) 667-749. https://doi.org/10.1016/S0045-6535(97)00195-1

[4]. J. Sun, X.Wu, J. Gan, Uptake and Metabolism of Phthalate Esters by Edible Plants. Environ. Sci. Technol. 49 (2015) 8472-8478. https://doi.org/10.1021/acs.est.5b01233

[5]. F. Shen, R.Liao, A. Ali, A.Mahar, D.Guo, R.Li, S.Xining,; M. K.Awasthi, Q.Wang, Z.Zhang, Spatial distribution and risk assessment of heavy metals in soil near a Pb/Zn smelter in Feng County, China. Ecotoxicol Environ Saf. 139 (2017) 254-262. https://doi.org/10.1016/j.ecoenv.2017.01.04462.

[6]. X. Zhu, J. Yao, F.Wang, Z.Yuan, J. Liu, G.Jordan, T. S. Knudsen, J. Avdalovic, Combined effects of antimony and sodium diethyldithiocarbamate on soil microbial activity and speciation change of heavy metals. Implications for contaminated lands hazardous material pollution in nonferrous metal mining areas. J. Hazard Mater. 349 (2018) 160-167. https://doi.org/10.1016/j.jhazmat.2018.01.044

[7]. C. Chen, H. Luan, Attention to toxic and hazardous sustances in benefition and metallurgy reagent. Mining metallurgy. 25-2 (2015) 67-70.

[8]. Y. Gao, T. An, Y. Ji,; G. Li, C. Zhao , Eco-toxicity and human estrogenic exposure risks from OH-initiated photochemical transformation of four phthalates in water: A computational study. Environ. Pollut. 206. (2015) 510-7. https://doi.org/10.1016/j.envpol.2015.08.006

[9]. L.Yu, H. X. Li, J. Y. Guo, Y. Q. Huang, H. Wang, M. Talukder, J. L. Li, Di (2-ethyl hexyl) phthalate (DEHP)-induced spleen toxicity in quail (Coturnix japonica) via disturbing Nrf2-mediated defense response. Environ. Pollut. 251 (2019) 984-989. https://doi.org/10.1016/j.envpol.2019.05.061

[10]. Y. Xu, S. H. Park, K. N.Yoon, S. J. Park, M. C. Gye, Effects of citrate ester plasticizers and bis (2-ethylhexyl) phthalate in the OECD 28-day repeated-dose toxicity test (OECD TG 407). Environ. Res. 172 (2019) 675-683. https://doi.org/10.1016/j.envres.2019.03.004

[11]. Y. Ding, Y. Liu, F. Fei, L. Yang, X. Wu, Study on the metabolism toxicity, susceptibility and mechanism of di-(2-ethylhexyl) phthalate on rat liver BRL cells with insulin resistance in vitro. Toxicology, 422 (2019) 102-120. https://doi.org/10.1016/j.tox.2019.05.011

[12]. Y. Tao, H. Li, J. Gu, H. Shi, S. Han, Y. Jiao, G. Zhong, Q. Zhang, M. S. Akindolie, Y. Lin, Z. Chen, Y. Zhang, Metabolism of diethyl phthalate (DEP) and identification of degradation intermediates by Pseudomonas sp. DNE-S1. Ecotoxicol. Environ. Saf. 173 (2019) 411-418. https://doi.org/10.1016/j.ecoenv.2019.02.055

[13]. V. Fernandez-Gonzalez, C. Moscoso-Perez, S. Muniategui-Lorenzo, P. Lopez-Mahia, PradaD.Rodriguez, Reliable, rapid and simple method for the analysis of phthalates in sediments by ultrasonic solvent extraction followed by head space-solid phase microextraction

gas chromatography mass spectrometry determination. Talanta. 162 (2017) 648-653. https://doi.org/10.1016/j.talanta.2016.10.068

[14]. T. H. A. Sr, Electronic code of federal regulations. Title 40-Protection of Environment. (1986) 98-99

[15]. M. A. Farajzadeh, S. M. Sorouraddin, A. Mogaddam, M. R, Microextraction methods for the determination of phthalate esters in liquid samples: A review. J. Sep. Sci. 38 (14) (2015) 2470-87. https://doi.org/10.1002/jssc.201500013

[16]. C. Ooka, H. Yoshida, M. Horio, K. Suzuki, T. Hattori, Adsorptive and photocatalytic performance of TiO2 pillared montmorillonite in degradation of endocrine disruptors having different hydrophobicity. Appl. Catal. B. 41, (3) (2003) 313-321. https://doi.org/ 10.1016/S0926-3373(02)00169-8

[17]. N. A. Medellin-Castillo, R. Ocampo-Perez, R. Leyva-Ramos, M. Sanchez-Polo, J. Rivera-Utrilla, J. D. Mendez-Diaz, Removal of diethyl phthalate from water solution by adsorption, photo-oxidation, ozonation and advanced oxidation process (UV/H2O2, O3/H2O2 and O3/activated carbon). Sci. Total. Environ. 442 (2013) 26-35. https://doi.org/10.1016/j.scitotenv.2012.10.062

[18]. N. A. Khan, B. K. Jung, Z. Hasan, S. H. Jhung, Adsorption and removal of phthalic acid and diethyl phthalate from water with zeolitic imidazolate and metal-organic frameworks. J. Hazard Mater. 282 (2015) 194-200. https://doi.org/10.1016/j.jhazmat.2014.03.047

[19]. J. Zhang, C. Zhang, Y. Zhu, J. Li, X. Li, Biodegradation of seven phthalate esters by Bacillus mojavensis B1811. Int. Biodeterior. Biodegrad. 132 (2018) 200-207. https://doi.org/10.1016/j.ibiod.2018.04.006

[20]. Y. Li, J. Gao, F. Meng,; J. Chi, Enhanced biodegradation of phthalate acid esters in marine sediments by benthic diatom Cylindrotheca closterium. Sci. Total. Environ. 508 (2015) 251-7. https://doi.org/10.1016/j.scitotenv.2014.12.002

[21]. B. V. Chang,; C. M. Yang,; C. H. Cheng,; S. Y. Yuan, Biodegradation of phthalate esters by two bacteria strains. Chemosphere. 55 (4) (2004) 533-538. https://doi.org/10.1016/j.chemosphere.2003.11.057

[22]. B. V. Chang, T. H. Wang, S. Y.Yuan, Biodegradation of four phthalate esters in sludge. Chemosphere. 69 (7) (2007) 1116-1123. https://doi.org/10.1016/j.chemosphere.2007.04.011

[23]. S.Y. Yuan, C. L., C.S. Liao , B.V. Chang , Occurrence and microbial degradation of phthalate esters in Taiwan river sediments. chemosphere. 49 (2002) 1295-1299. https://doi.org/10.1016/s0045-6535(02)00495-2

[24]. D Colin. Cartwright, P Ian. Thompson, G Richard. Burns, Degradation and impact of phthalate plasticizers on soil microbial communities. Environ. Toxicol. Chem.. 19 (2000) 1253-1261. https://doi.org/10.1002/etc.5620190506

[25]. Y. Wang, H. Liu, Y. Peng, Tong, L.; L. Feng, K. Ma, New pathways for the biodegradation of diethyl phthalate by Sphingobium yanoikuyae SHJ. Process Biochem.. 71 (2018) 152-158. https://doi.org/ 10.1016/j.procbio.2018.05.010

[26]. X. Zhang, M. Feng, R. Qu, H. Liu, L. Wang, Z. Wang, Catalytic degradation of diethyl phthalate in aqueous solution by persulfate activated with nano-scaled magnetic CuFe 2 O 4 /MWCNTs. Chem. Eng. J. 301 (2016) 1-11. https://doi.org/10.1016/j.cej.2016.04.096

[27]. G. P. Yang, X. K. Zhao, X. J. Sun, X. L. Lu, Oxidative degradation of diethyl phthalate by photochemically-enhanced Fenton reaction. J. Hazard Mater. 126 (1-3), (2005) 112-8. https://doi.org/ 10.1016/j.jhazmat.2005.06.014

[28]. B. Xu, N. Y. Gao, X. F. Sun, S. J. Xia, M. Rui, M. O. Simonnot, C. Causserand, J. F. Zhao, Photochemical degradation of diethyl phthalate with UV/H2O2. J. Hazard Mater. 139 (1) (2007)132-9. https://doi.org/10.1016/j.jhazmat.2006.06.026

[29]. Y. Wu,; L. Deng,; L. Bu,; S. Zhu,; Z. Shi,; S. Zhou, Degradation of diethyl phthalate (DEP) by vacuum ultraviolet process: influencing factors, oxidation products, and toxicity assessment. Environ. Sci. Pollut. Res Int. 26 (6) (2019)5435-5444. https://doi.org/10.1007/s11356-018-3914-x

[30]. G. Wen, J. Ma, Z. Q.Liu, L. Zhao, Ozonation kinetics for the degradation of phthalate esters in water and the reduction of toxicity in the process of O3/H2O2. J. Hazard. Mater. 195 (2011) 371-7. https://doi.org/10.1016/j.jhazmat.2011.08.054

[31]. S. Wei, V. Pintus, M. Schreiner, Photochemical degradation study of polyvinyl acetate paints used in artworks by Py-GC/MS. J. Anal. Appl. Pyrolysis. 97 (5) (2012) 158-163. https://doi.org/ 10.1016/j.jaap.2012.05.004

[32]. S. Na, Y. G. Ahn, M. Cui, J. Khim, Significant diethyl phthalate (DEP) degradation by combined advanced oxidation process in aqueous solution. J. Environ. Manage. 101 (2012) 104-10. https://doi.org/ 10.1016/j.jenvman.2012.01.028

[33]. I. Gultekin,; N. H. Ince, Synthetic endocrine disruptors in the environment and water remediation by advanced oxidation processes. J. Environ. Manage. 85 (4) (2007) 816-32. https://doi.org/ 10.1016/j.jenvman.2012.01.028

[34]. G. Fang, C. Zhu, D. D.Dionysiou, J. Gao, D. Zhou, Mechanism of hydroxyl radical generation from biochar suspensions: Implications to diethyl phthalate degradation. Bioresour. Technol. 176 (2015) 210-7. https://doi.org/10.1016/j.biortech.2014.11.032

[35]. T. F.de Oliveira, O. Chedeville, H. Fauduet, B. Cagnon, Use of ozone/activated carbon coupling to remove diethyl phthalate from water: Influence of activated carbon textural and chemical properties. Desalination. 276 (1-3) (2011) 359-365. https://doi.org/10.1016/j.desal.2011.03.084

[36]. D. Zhang, L. Wu, J. Yao, H. Herrmann,; H.-H. Richnow, Carbon and hydrogen isotope fractionation of phthalate esters during degradation by sulfate and hydroxyl radicals. Chem. Eng. J. 347 (2018) 111-118. https://doi.org/10.1016/j.cej.2018.04.047

[37]. I. Hussain, Y. Zhang, S. Huang, X. Du, Degradation of p-chloroaniline by persulfate activatedwith zero-valent iron. Chem. Eng. J. 203 (2012) 269-276. https://doi.org/ 10.1016/j.cej.2012.06.120

[38]. Y. Li, X. Yuan, Z. Wu, H. Wang, Z. Xiao, Y. Wu, X. Chen, G. Zeng, Enhancing the sludge dewaterability by electrolysis/electrocoagulation combined with zero-valent iron activated persulfate process. Chem. Eng. J. 303 (2016) 636-645. https://doi.org/10.1016/j.cej.2016.06.041

[39]. O. S. Furman，A. L. Teel, R. J. Watts, Mechanism of Base Activation of Persulfate. Environ. Sci. Technol. (2010) 6423–6428. https://doi.org/10.1021/es1013714

[40]. S. Y. Oh, H. W. Kim, J. M. Park, H. S.Park, C.Yoon, Oxidation of polyvinyl alcohol by persulfate activated with heat, Fe2+, and zero-valent iron. J. Hazard Mater. 168 (2009) 346-51. https://doi.org/ 10.1016/j.jhazmat.2009.02.065

[41]. A. Tsitonaki, B. Petri, M.Crimi, H. MosbEK, R. L. Siegrist, P. L. Bjerg, In Situ Chemical Oxidation of Contaminated Soil and Groundwater Using Persulfate: A Review. Critical Reviews in Environ. Sci. and Technol. 40 (1) (2010) 55-91. https://doi.org/ 10.1080/10643380802039303

[42]. H. Li, J. Wan, Y. Ma, Y. Wang, Reaction pathway and oxidation mechanisms of dibutyl phthalate by persulfate activated with zero-valent iron. Sci. Total. Environ. 562 (2016) 889-897. https://doi.org/ 10.1016/j.scitotenv.2016.04.093

[43]. S. O. Furman, A. L. T, R. J. Watts, Mechanism of Base Activation of Persulfate. Environ. Sci. Technol. 44 (2010) 6423–6428. https://doi.org/10.1021/es1013714

[44]. X. Zhu, X Wu, J. Yao, F Wang, W. Liu, Y. Luo, X. Jiang, Toxic effects of binary toxicants of cresol frother and Cu (II) on soil microorganisms. Int. Biodeterior. Biodegrad. 128 (2018) 155-163. https://doi.org/10.1016/j.ibiod.2017.04.012

[45]. N. Zhang, S. Bashir, J. Qin, J. Schindelka, A. Fischer, I. Nijenhuis, H. Herrmann, L. Y. Wick, H. H. Richnow, Compound specific stable isotope analysis (CSIA) to characterize transformation mechanisms of alpha-hexachlorocyclohexane. J. Hazard Mater. 280 (2014) 750-7. https://doi.org/10.1016/j.jhazmat.2014.08.046

[46]. L. Wu, D. Verma, M. Bondgaard, A. Melvej, C.Vogt, S. Subudhi, H. H. Richnow, Carbon and hydrogen isotope analysis of parathion for characterizing its natural attenuation by hydrolysis at a contaminated site. Water. Res. 143 (2018) 146-154. https://doi.org/10.1016/j.watres.2018.06.039

[47]. L.Wu, S. Kummel, H. H. Richnow, Validation of GC-IRMS techniques for delta13C and delta2H CSIA of organophosphorus compounds and their potential for studying the mode of hydrolysis in the environment. Anal. Bioanal. Chem. 409 (10) (2017) 2581-2590. https://doi.org/10.1007/s00216-017-0203-3

[48]. N. Zhang, I. Geronimo, P. Paneth, J. Schindelka, T. Schaefer, H. Herrmann, C. Vogt, H. H. Richnow, Analyzing sites of OH radical attack (ring vs. side chain) in oxidation of substituted benzenes via dual stable isotope analysis (δ(13)C and δ(2)H). Sci. Total. Environ. 542 (2016) (Pt A), 484-94. https://doi.org/ 10.1016/j.scitotenv.2015.10.075

[49]. A. Zelmer, N. Zhang, K. Kominkova, D. Nachtigallova, H. H. Richnow, P. Klan, Photochemistry of 4-chlorophenol in liquid and frozen aqueous media studied by chemical, compound-specific isotope, and DFT analyses. Langmuir. 31 (39) (2015) 10743-50. https://doi.org/ 10.1021/acs.langmuir.5b02990

[50]. D. Zhang, L. Wu, J. Yao, C.Vogt, H. H. Richnow , Carbon and hydrogen isotopic fractionation during abiotic hydrolysis and aerobic biodegradation of phthalate esters. Sci. Total. Environ. 660 (2019) 559-566. https://doi.org/10.1016/j.scitotenv.2019.01.003

[51]. Y. S. Shao, N. Y. Xian, Z. Y. Wang, Degradation kinetic of phthalate esters and the formation of brominated byproducts in heat-activated persulfate system. Chem. Eng. J. 359(2018) 1086-1096. https://doi.org/10.1016/j.cej.2018.11.075

[52]. W. Li, H. Guo, C. Wang，Y. Zhang, E. Du, ROS reevaluation for degradation of 4-chloro-3,5-dimethylphenol (PCMX) by UV and UV/persulfate processes in the water: Kinetics,

mechanism, DFT studies and toxicity evolution. Chem. Eng. J. 390(2020) 124610. https://doi.org/10.1016/j.cej.2020.124610

[53]. N, Wahba, M.F.E.A, M. EL Sadr. Iodometric Method for Determination of Persulfates. Anal. Chem. 31(1959) 1870-1871. https://doi.org/10.1021/ac60155a059

[54]. H. Liu, Z. Wu, X. Huang, C.Yarnes, M. Li, L. Tong, Carbon isotopic fractionation during biodegradation of phthalate esters in anoxic condition. Chemosphere. 138 (2015) 1021-7. https://doi.org/ 10.1016/j.chemosphere.2014.12.063

[55]. S. i. Mizushima, Y. Morino, M. Takeda, Molecular Configurations in Rotational Isomerism. The Journal of Chem. Phy. 9 (1941) 826-826. https://doi.org/ 10.1016/j.chemosphere.2014.12.063

[56]. E. Martin, L Zwank, D Hunkeler,P. R. Schwarzenbach. A New Concept Linking Observable Stable Isotope Fractionation to Transformation Pathways of Organic Pollutants. Environ. Sci. Technol. 39. (2005) 6896-6916. https://doi.org/10.1021/es0504587

[57]. X. M. Liang, Y.R. Dong, T. KuderU, L. R. Krumholz, R. P. Philp, C. E. Butler, Distinguishing abiotic and biotic transformation of tetrachloroethylene and trichloroethylene by stable carbon isotope fractionation. Environ. Sci. Technol. 41. (2007) 7094-7100. https://doi.org/10.1021/es070970n

[58]. M. Nie, C. Yan,; M. Li, X. Wang, W. Bi, W. Dong, Degradation of chloramphenicol by persulfate activated by Fe2+ and zerovalent iron. Chem. Eng. J. 279 (2015) 507-515. https://doi.org/10.1016/j.cej.2015.05.055

[59]. Y. F. Rao, L. Qu, H. Yang, W. Chu, Degradation of carbamazepine by Fe(II)-activated persulfate process. J. Hazard Mater. 268 (2014) 23-32. https://doi.org/10.1016/j.jhazmat.2014.01.010

[60]. D. Han, J. Wan, Y. Ma, Y. Wang,; Y. Li, D. Li, Z. Guan, New insights into the role of organic chelating agents in Fe(II) activated persulfate processes. Chem. Eng. J. 269 (2015) 425-433.https://doi.org/10.1016/j.cej.2015.01.106

[61]. C.J Liang., H. W. Su, Identification of Sulfate and Hydroxyl Radicals in Thermally Activated Persulfate. Ind. Eng. Chem. Res. 48. (2009) 5558–5562. https://doi.org/10.1021/ie9002848

[62]. X. Wu, X. Gu, S. Lu, M. Xu, X. Zang, Z. Miao, Z. Qiu, Q. Sui, Degradation of trichloroethylene in aqueous solution by persulfate activated with citric acid chelated ferrous ion. Chem. Eng. J. 255 (2014) 585-592. https://doi.org/10.1016/j.cej.2014.06.085

[63]. X. Jiang, Y. Wu, P. Wang, H. Li, W. Dong, Degradation of bisphenol A in aqueous solution by persulfate activated with ferrous ion. Environ. Sci. Pollut. Res. Int. 20 (7) (2013) 4947-53. https://doi.org/10.1007/s11356-013-1468-5

[64]. P. Neta, R. E.Huie, A. B. Ross, Rate Constants for Reactions of Peroxyl Radicals in Fluid Solutions. J. Phys. Chem. Ref. Data. 12 (2) (1990) 413. https://doi.org/ 10.1007/s11356-013-1468-5

[65]. G. P. Anipsitakis, D. D. Dionysiou., Radical Generation by the Interaction of Transition Metals with Common Oxidants. Environ. Sci. Technol. 38. (2004)3705-3712. https://doi.org/ 10.1021/es035121o

[66]. Y. Wang , H. Sun, X. Duan, A new magnetic nano zero-valent iron encapsulated in carbon spheres for oxidative degradation of phenol. Appl. Catal. B-Environ. (2015) 172-173, 73-81. https://doi.org/10.1016/j.apcatb.2015.02.016

[67]. Y. Wang, S. Hun, H M. Ang, 3D-hierarchically structured MnO2 for catalytic oxidation of phenol solutions by activation of peroxymonosulfate Structure dependence and mechanism. Appl. Catal. B-Environ.. 164 (2015) 159-167. https://doi.org/10.1016/j.apcatb.2014.09.004

[68]. L. Fang, K. Liu, F. Li, W. Zeng, Y. Ma, New insights into stoichiometric efficiency and synergistic mechanism of persulfate activation by zero-valent bimetal (Iron/Copper) for organic pollutant degradation. J Hazard Mater, 403(2021) 123669. https://doi.org/ 10.1016/j.jhazmat.2020.123669

[69]. Q. Zhong, Q. Lin, R. Huang, H. Fu, R. Xiao, Oxidative degradation of tetracycline using persulfate activated by N and Cu codoped biochar. Chem. Eng. J. 380(2020) 122608. https://doi.org/10.1016/j.cej.2019.122608

[70]. Y. Liu, Y. Zhang, B. Wang, S. Wang, A. Qadeer, Degradation of ibuprofen in soil systems by persulfate activated with pyrophosphate chelated Fe(II). Chem. Eng. J. 379(2020) 122145. https://doi.org/10.1016/j.cej.2019.122145

[71]. K. S. Tay, N. A. Rahman, M. R. B. Abas, Fenton degradation of dialkylphthalates: products and mechanism. Environ. Chem. Lett. 9 (4) (2011) 539-546. https://doi.org/ 10.1007/s10311-011-0317-3

[72]. T.C. An, Y. G., G. Y. Li, P. V. Kamat, J. Peller, and M. V. Joyce, Kinetics and Mechanism of •OH Mediated Degradation of Dimethyl Phthalate in Aqueous Solution Experimental and Theoretical Studies. Environ. Sci. Technol. 48(2013) 641−648. https://doi.org/10.1021/es404453v

[73]. T. C. An, Y. P. Gao, G.Y. Li, P. V. Kamat, J. Peller, M. V. Joyce, Kinetics and Mechanism of •OH Mediated Degradation of Dimethyl Phthalate in Aqueous Solution: Experimental and Theoretical Studies. Environ. Sci. Technol. 48 (2013) 641-648. https://doi.org/ 10.1021/es404453v

Table 1: Degradation kinetic parameters of DEP during chemical oxidation.

pH	Concentration of ZVI (g L^{-1})	Dominant radical/s	k (h^{-1})	Half-life (h)	R^2
3	0.2	•OH	0.0035	285.71	0.9587
	0.5	•OH	0.0095	105.26	0.9574
	1	•OH	0.0301	33.22	0.947
7	0.2	•OH	0.0057	175.44	0.9639
	0.5	•OH	0.0115	86.96	0.9721
	1	•OH	0.0306	32.68	0.9895
11	0.2	•OH	0.0034	294.12	0.976
	0.5	•OH	0.0044	227.27	0.9748
	1	•OH	0.0204	49.02	0.9337
11	-	-	0.0028	357.14	0.9600

Table 2 Isotope fractionation parameters of DEP during chemical oxidation.

pH	Concentration of **ZVI (g/l)**	εC (‰)	R^2	Average (εC (‰))	εH (‰)	R^2	Average (εH (‰))	Λ	Average (Λ)
	0.2	-1.1±0.21	0.9673		-10.2±3.6	0.9283		15.1±4.2	
3	0.5	-0.8±0.20	0.9800	0.79±0.45	- 8.7±5.1	0.9314	8.97±4.87	12.7±3.5	13.3±3.4
	1.0	-0.6±0.36	0.9698		-8.5±3.3	0.9731		11.7±2.6	
	0.2	-1.10±0.01	0.9808		-14.0±4.1	0.9352		10.9±2.9	
7	0.5	-1.11±0.01	0.9810	1.10±0.45	-11.6±5.5	0.9598	13.10±5.60	11.1±4.2	11.2±3.6
	1.0	-1.00±0.01	0.9853		-13.7±3.2	0.9258		11.6±3.6	
	0.2	-1.48±0.21	0.9813		-23.0±3.2	0.9612		15.0±3.1	
11	0.5	-1.18±0.20	0.9715	3.10±0.60	-19.2±4.6	0.9651	18.02±5.01	12.0±2.9	13.3±2.9
	1.0	-0.77±0.16	0.9623		-14.0±2.1	0.9205		12.8±2.8	
11	Hydrolysis experiment	-5.90±0.71	0.9600		n.d.		n.d.		

[a] Uncertainty given as 95% confidence interval, n.d. no fractionation detected.

Table 3 Comparison of the current results with others

	K	R^2	^{13}C	R^2	^{2}H	R^2	Λ	reference
pH 2_PS	0.0057	0.999	−1.39± 0.13	0.995	−41.8 ± 2.4	0.998	25.7 ± 2.6	[36]
pH 7 PS	0.0025	0.973	−1.57± 0.18	0.993	−28.3 ± 3.3	0.993	14.9 ±3.0	[36]
pH 7_UV/H_2O_2	0.0541	0.993	−2.30± 0.42	0.990	−6.8 ± 1.3	0.989	2.4 ± 0.2	[36]
pH 3_PS/ZVI(0.2)	0.0035	0.9587	-1.1±0.21	0.9673	-10.2±3.6	0.9283	15.1±4.2	This study
pH 3_PS/ZVI(0.5)	0.0095	0.9574	-0.8±0.20	0.9800	- 8.7±5.1	0.9314	12.7±3.5	This study
pH 3_PS/ZVI(1.0)	0.0301	0.947	-0.6±0.36	0.9698	-8.5±3.3	0.9731	11.7±2.6	This study
pH 7_PS/ZVI(0.2)	0.0057	0.9639	-1.10±0.01	0.9808	-14.0±4.1	0.9352	10.9±2.9	This study
pH 7_PS/ZVI(0.5)	0.0115	0.9721	-1.11±0.01	0.9810	-11.6±5.5	0.9598	11.1±4.2	This study
pH 7_PS/ZVI(1.0)	0.0306	0.9895	-1.00±0.01	0.9853	-13.7±3.2	0.9258	11.6±3.6	This study
pH 11_PS/ZVI(0.2)	0.0034	0.976	-1.48±0.21	0.9813	-23.0±3.2	0.9612	15.0±3.1	This study

pH 11_PS/ZVI(0.5)	0.0044	0.9748	-1.18±0.20	0.9715	-19.2±4.6	0.9651	12.0±2.9	This study
pH 11_PS/ZVI(1.0)	0.0204	0.9337	-0.77±0.16	0.9623	-14.0±2.1	0.9205	12.8±2.8	This study

[a] Uncertainty given as 95% confidence interval

Table 4. Summary of results from DEP degradation by PS activated with ZVI: identification of primary radical species

pH	Reaction rate of DEP degradation	inhibition on the k_{obs} with addition of		Major free radical species
		EtOH	TBA	
3	0.0095	0.0018	0.0021	•OH
7	0.0115	0.0016	0.0018	•OH
11	0.0044	0.0004	0.0005	•OH

Table 5 Carbon and hydrogen AKIEs of DEP for investigated experimental systems.

pH	εC (‰)	^{13}C- AKIE	εH (‰)	^{2}H- AKIE
	-1.1±0.21	1.02	-10.2±3.6	1.16
3	-0.8±0.20	1.01	- 8.7±5.1	1.14
	-0.6±0.36	1.01	-8.5±3.3	1.14
	-1.10±0.01	1.02	-14.0±4.1	1.24
7	-1.11±0.01	1.01	-11.6±5.5	1.14
	-1.00±0.01	1.01	-13.7±3.2	1.20
	-1.48±0.21	1.02	-23.0±3.2	1.40
11	-1.18±0.20	1.02	-19.2±4.6	1.37
	-0.77±0.16	1.01	-14.0±2.1	1.24

[a] Uncertainty given as 95% confidence interval

List of Figures

Fig. 1. Effect of the concentration of zero-valent iron on the degradation rate of DEP in ZVI/PS system at pH 3, 7 and 11; $[DEP]_0$ = 0.8 mM; $[PS]_0$ = 80 Mm; $[Fe]_0$=0.2 0.5/1 g L^{-1}.

Fig. 2. The concentration of persulfate in the presence of nZVI but without DEP present; $[PS]_0$ = 80 mM; $[Fe]_0$=0.5 g L^{-1}.

Fig. 3. The concentration of persulfate in the studied conditions (pH=3, pH=7 and pH=11). $[DEP]_0$=0.8 Mm; $[PS]_0$ = 80 mM; $[Fe]_0$=0.5 g L^{-1}

Fig. 4. The concentration of Fe^{2+} in the studied conditions (pH=3, pH=7 and pH=11). $[DEP]_0$=0.8 Mm; $[PS]_0$ = 80 mM; $[Fe]_0$=0.5 g L^{-1}

Fig. 5. Rayleigh regression of carbon (left panels, A, C, E) and hydrogen (right panels, B, D, F) isotope data during DEP oxidation in ZVI/PS system with different amount of ZVI (0.2, 0.5 and 1.0 g L^{-1})

Fig. 6. Correlation of ^{2}H and ^{13}C isotope fractionation for DEP during DEP oxidation in ZVI/PS system with different amount of ZVI at different pH value. The Λ values are shown in Table. 2.

Fig. 7. Degradation kinetic curves of DEP during the study of radical quenching at pH 3, pH 7 and pH 11. Experiment condition: DEP = 0. 8 mM; PS = 80 mM; ZVI =0.5 g L^{-1}; EtOH = 400 mM; TBA = 400 mM.

Fig. 8. Electron paramagnetic resonance (EPR) spectra of pH=3, pH=7, pH=11. ZVI/PS/DEP system. Experiment condition: DEP = 0. 8 mM; PS = 80 mM; ZVI =0.5 g L^{-1}.

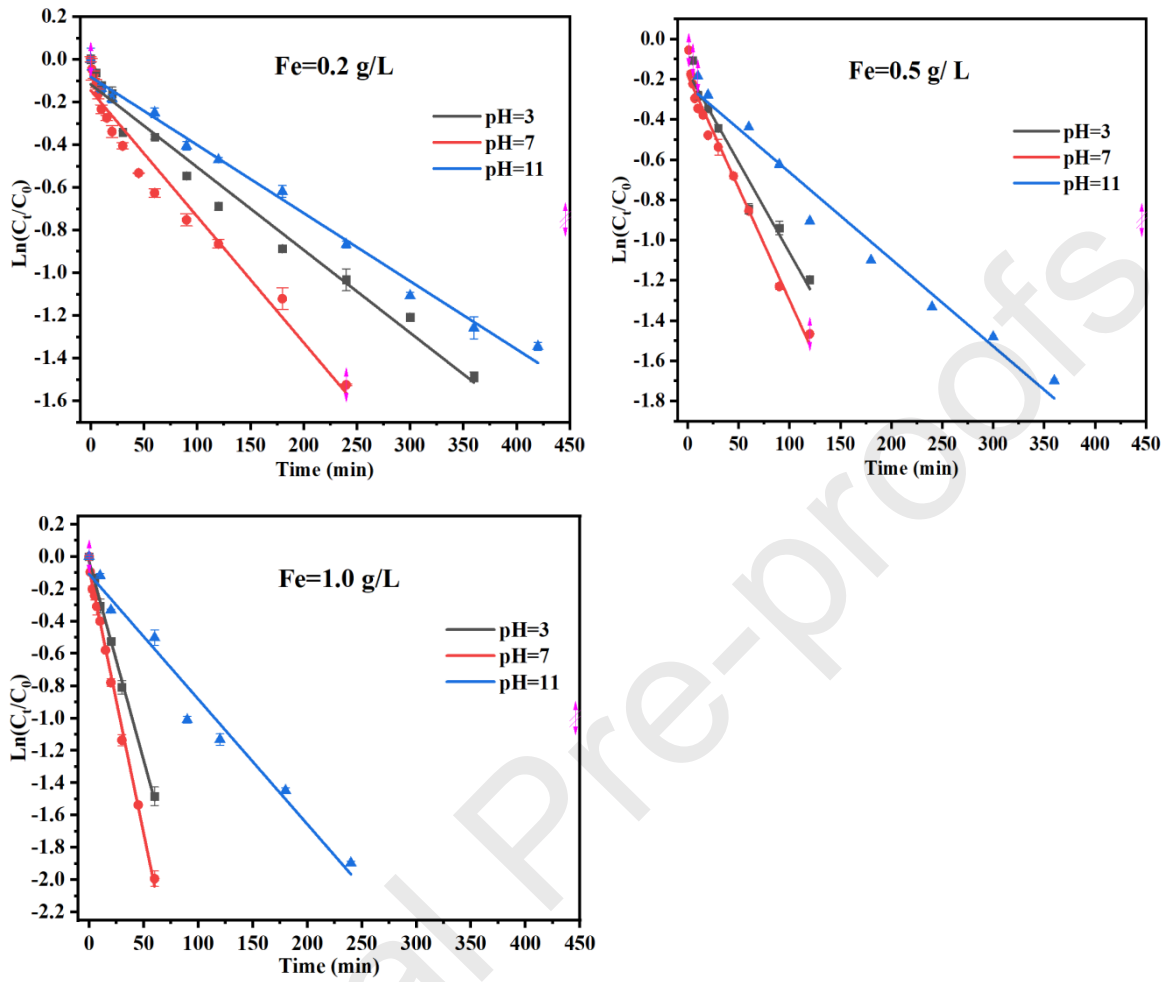

Fig. 1. Effect of the concentration of zero-valent iron on the degradation rate of DEP in ZVI/PS system at pH 3, 7 and 11. $[DEP]_0$ = 0.8 mM; $[PS]_0$ = 80 mM; $[Fe]_0$=0.2/0.5/1 g L^{-1}

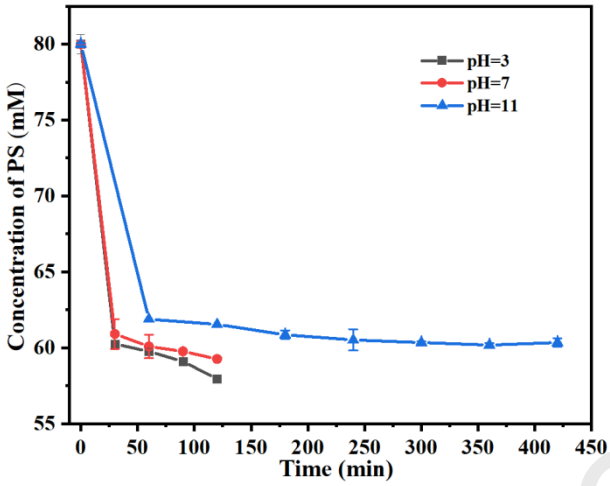

Fig. 2. The concentration of persulfate in the presence of nZVI but without DEP

present $[PS]_0$ = 80 mM; $[Fe]_0$=0.5 g L^{-1}

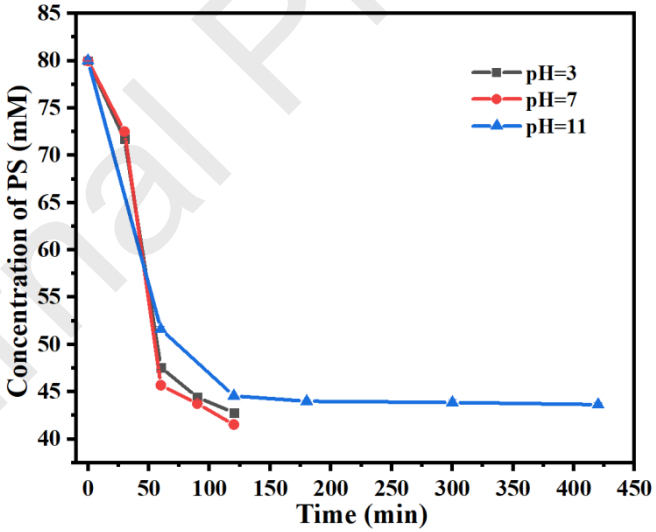

Fig. 3. The concentration of persulfate in the studied conditions (pH=3, pH=7 and

pH=11). $[DEP]_0$=0.8 Mm; $[PS]_0$ = 80 mM; $[Fe]_0$=0.5 g L^{-1}

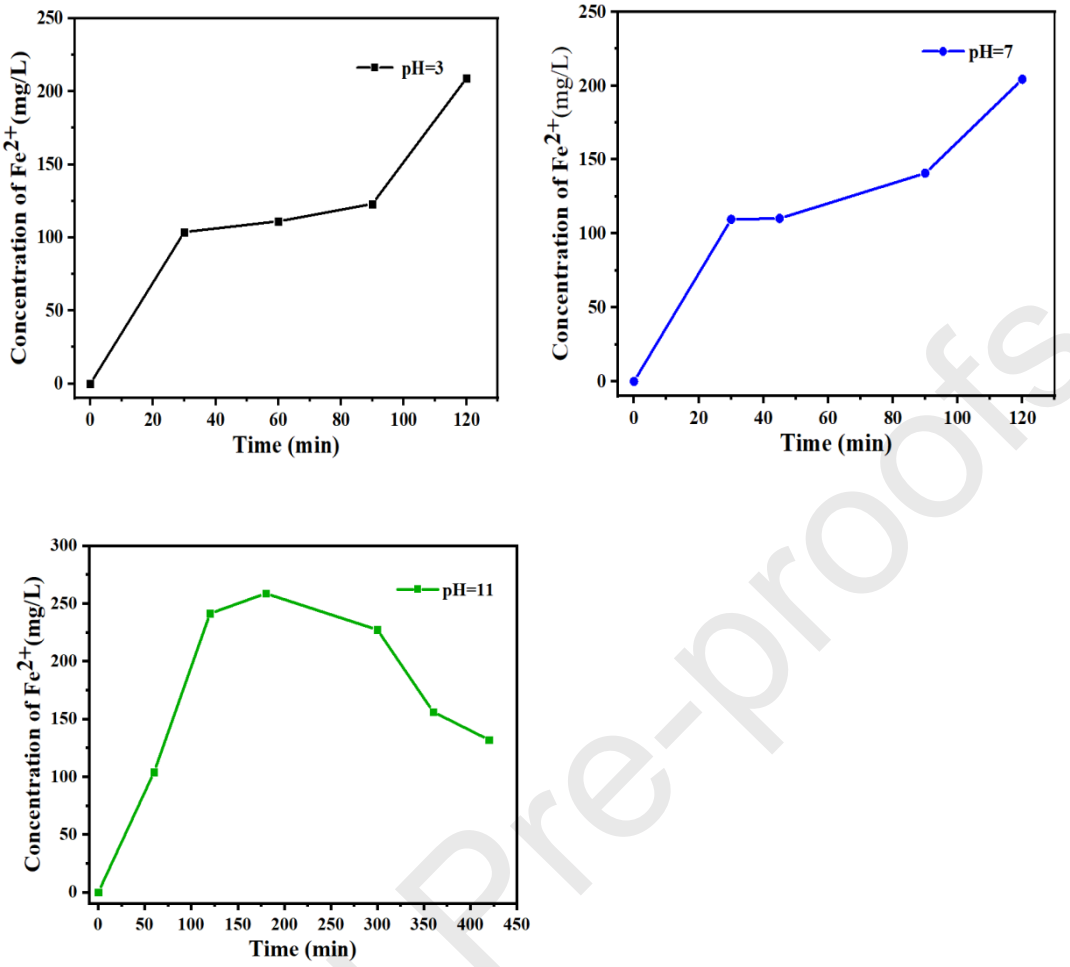

Fig. 4. The concentration of Fe^{2+} in the studied conditions (pH=3, pH=7 and pH=11).

$[DEP]_0$=0.8 Mm; $[PS]_0$ = 80 mM; $[Fe]_0$=0.5 g L^{-1}

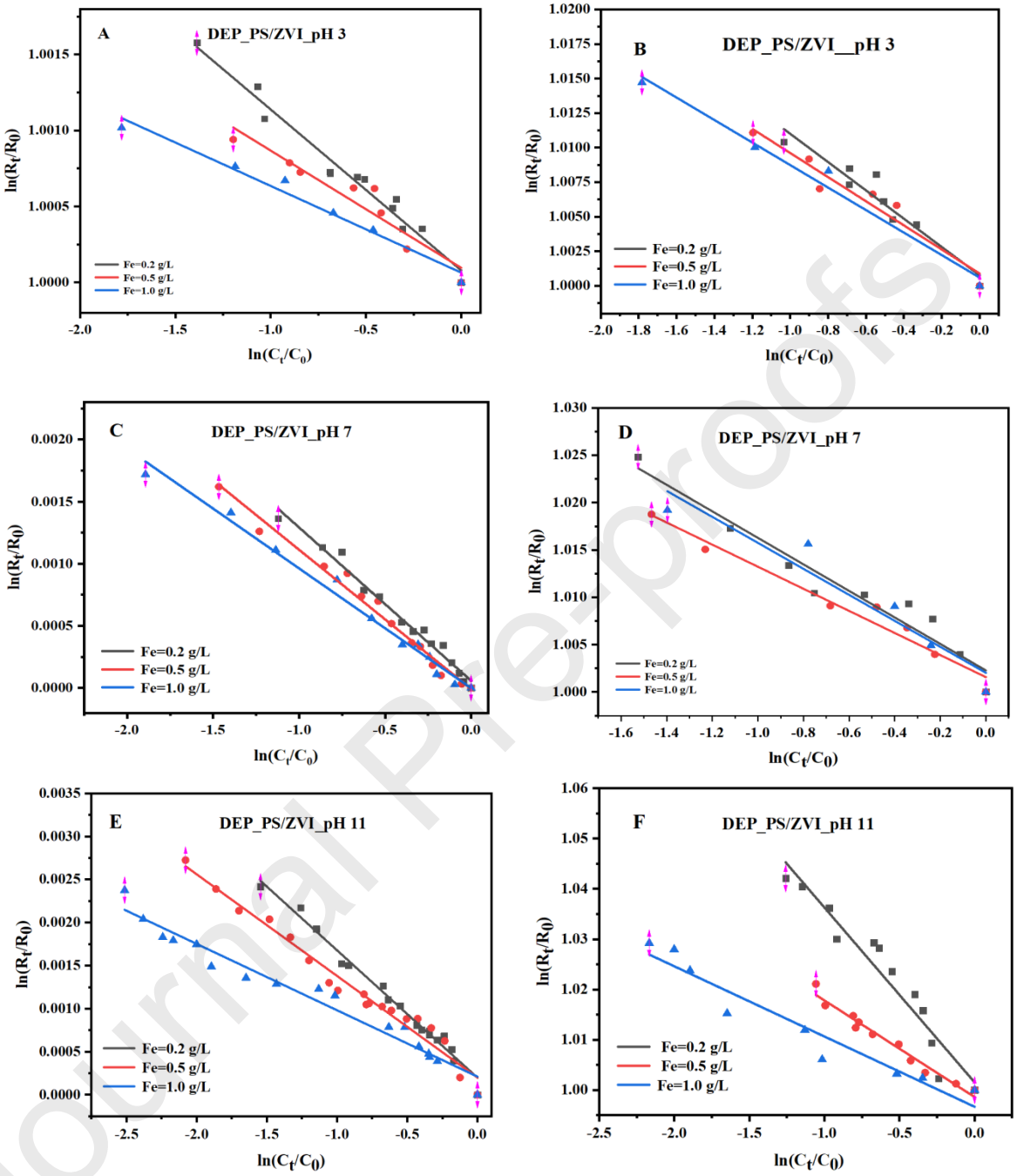

Fig. 5. Rayleigh regression of carbon (left panels, A, C, E) and hydrogen (right panels, B, D, F) isotope data during DEP oxidation in ZVI/PS system with different amount of ZVI (0.2,0.5 and 1.0 g L^{-1}).

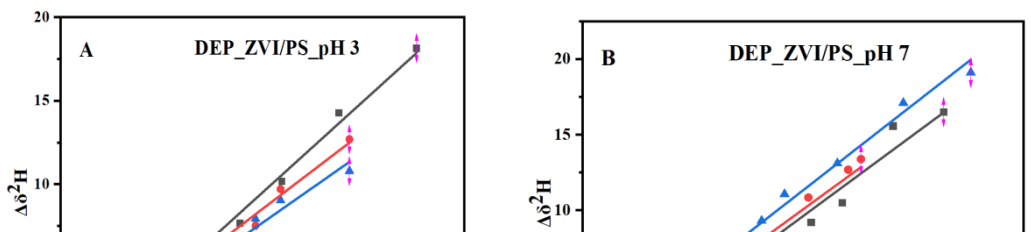

Fig. 6. Correlation of ^{2}H and ^{13}C isotope fractionation for DEP during DEP oxidation in ZVI/PS system with different amount of ZVI at different pH value. The Λ values are shown in Table. 2.

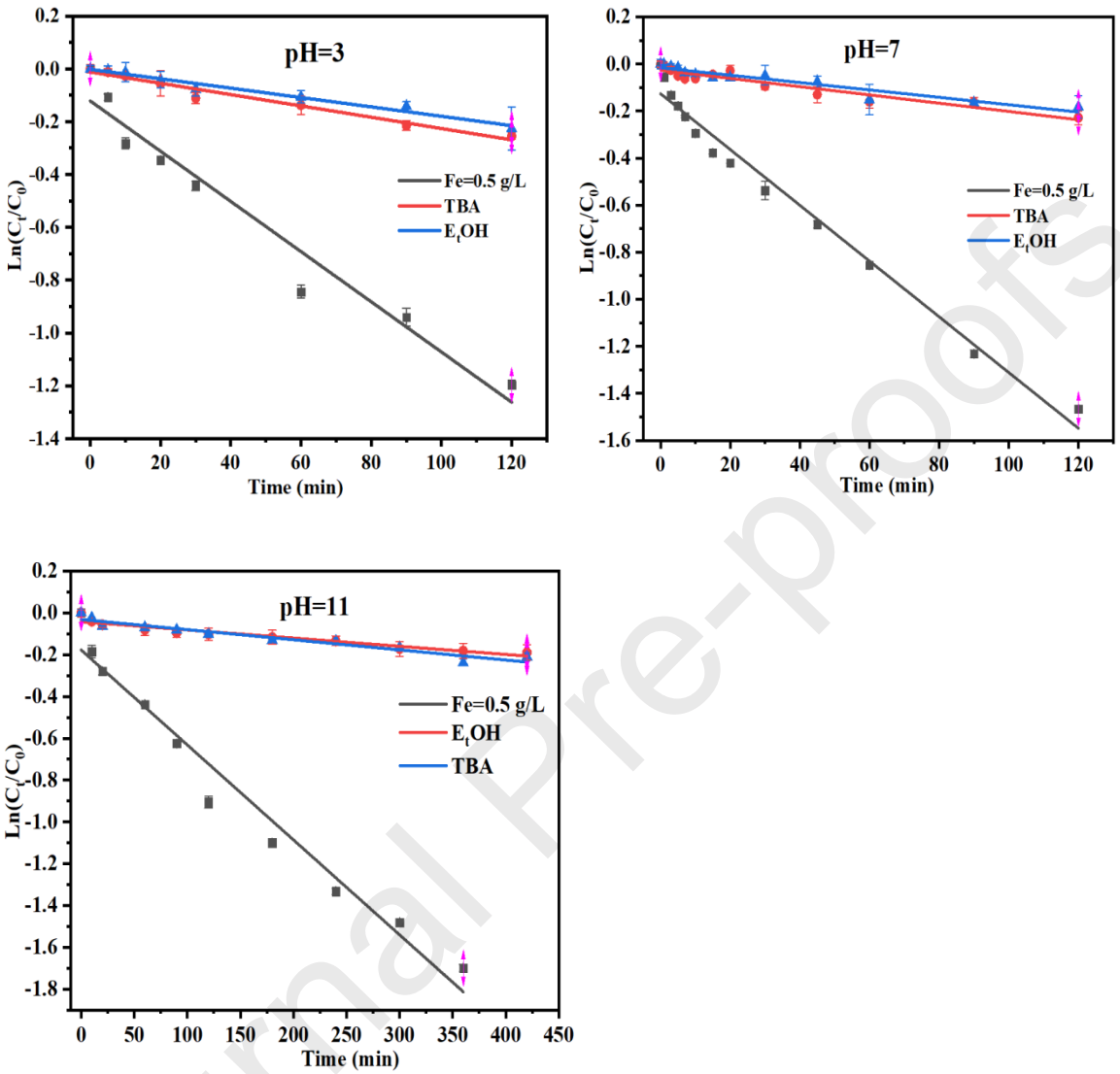

Fig. 7. Degradation kinetic curves of DEP during the study of radical quenching at pH 3, pH 7 and pH 11. Experiment condition: DEP = 0. 8 mM; PS = 80 mM; ZVI =0.5 g L^{-1}; EtOH = 400 mM; TBA = 400 mM.

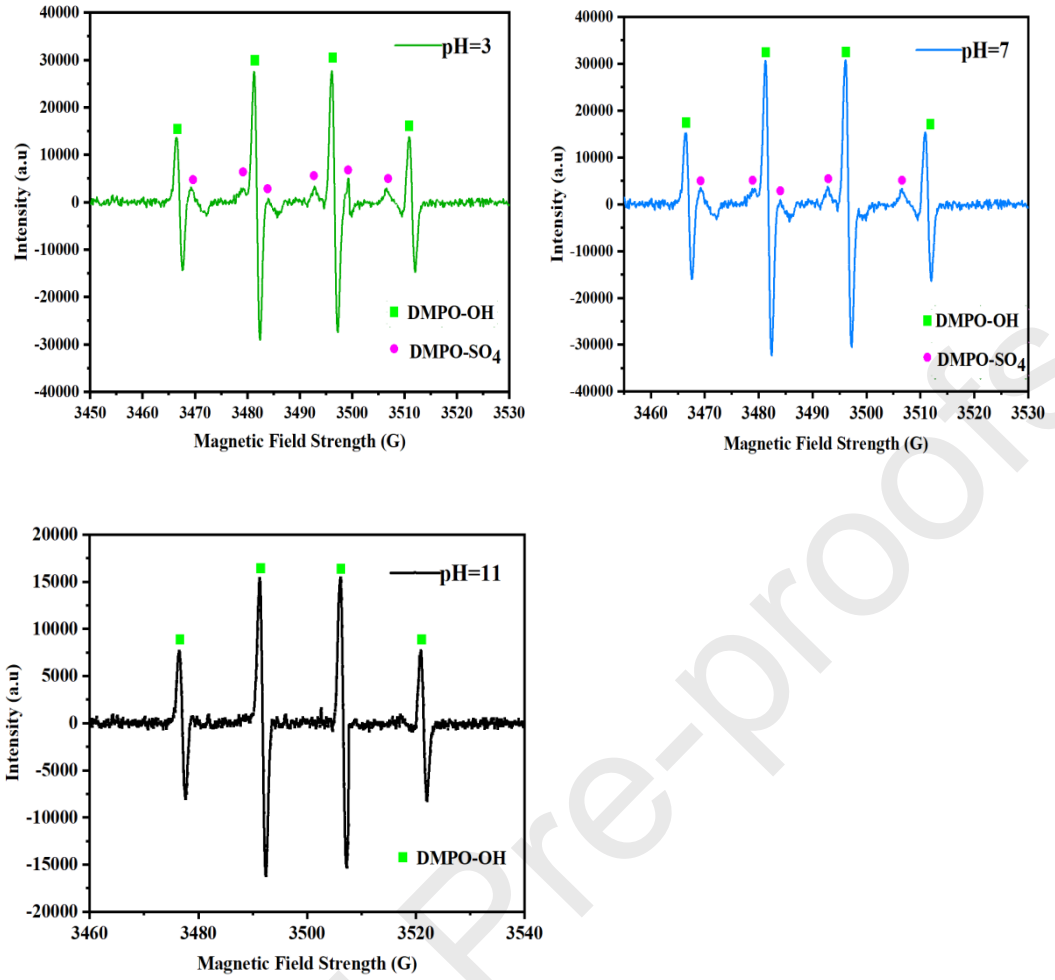

Fig. 8. Electron paramagnetic resonance (EPR) spectra of pH=3, pH=7, pH=11 ZVI/PS/DEP system. Experiment condition: DEP = 0. 8 mM; PS = 80 mM; ZVI =0.5 g L^{-1};

Research Highlights

- Degradation of DEP in the PS/ZVI was studied at different pHs.
- Isotope fractionation was used to understand the DEP oxidation pathway.
- •OH was found to be the main functioning radical species at pH=3 and 7.
- •OH was the predominant species for PS/ZVI oxidation of DEP at pH=11.

- •OH addition to the DEP ring is assumed to be the main reaction mechanism.